

## Synporins—synthetic proteins that emulate the pore structure of biological ionic channels

MAURICIO MONTAL<sup>§¶</sup>, MYRTA S. MONTAL<sup>§</sup>, AND JOHN M. TOMICH<sup>¶¶</sup>

<sup>§</sup>Departments of Biology and Physics, University of California, San Diego, La Jolla, CA 92093-0319; and <sup>¶¶</sup>Medical Genetics Division, Children's Hospital, Los Angeles, CA 90027

Communicated by Bruno Zimm, May 3, 1990 (received for review February 27, 1990)

**ABSTRACT** A class of proteins that mimic the fundamental pore structure of authentic ionic channels has been designed, synthesized, and characterized. The design is based on our earlier result that a 23-mer peptide with the sequence of the M2 segment of the *Torpedo californica* acetylcholine receptor  $\delta$  subunit—Glu-Lys-Met-Ser-Thr-Ala-Ile-Ser-Val-Leu-Leu-Ala-Gln-Ala-Val-Phe-Leu-Leu-Leu-Thr-Ser-Gln-Arg—forms cation-selective channels in lipid bilayers, presumably by self-assembly of conductive oligomers. Accordingly, a tethered parallel tetramer was synthesized with four M2 $\delta$  peptides attached to a carrier template—a 9-amino acid backbone with four attachment sites. As expected, the complete 101-residue protein does form channels in lipid bilayers reproducing several features that are characteristic of authentic acetylcholine receptor channels, such as single-channel conductance, cation selectivity, transitions between closed and open states in the millisecond time range, and sensitivity to local anesthetic channel blockers. An analogue protein, in which the serine residue in position 8 is replaced with alanine in each of the four M2 $\delta$  23-mer peptides ([Ala<sup>8</sup>]M2 $\delta$ ), also forms channels that, however, exhibit lower single-channel conductance. By contrast, a similar tethered tetramer with M1 $\delta$  peptides does not form channels, in accord with expectations. The general validity of this strategy to other channel sequences and oligomer numbers is anticipated. Thus, synporins—a term coined to identify this class of synthetic pore proteins—enrich our armamentarium directed toward the elucidation of structure-function relationships.

Ionic channels are transmembrane protein arrays organized around a central aqueous pore (for review, see ref. 1). A key issue has been to account for the known permeation properties of channels, specifically the pore size and ionic selectivity of the open channel, in terms of structural elements predicted from the deduced amino acid sequences.

In one approach to this problem, a hypothesis is first formulated about the existence of such functional segments. The design of a functional peptide that mimics the predicted structural element is followed by its chemical synthesis using solid-phase methods, and the peptide's ability to form ion channels is tested by incorporating it into a synthetic lipid bilayer. The channel activity of the peptide is characterized in terms of ion conduction and channel gating. This characterization is compared with the specific features of the authentic channel. The comparison, in turn, leads to a redesign of the peptide to match the anticipated characteristics of the authentic channel. Finally, the identification of a specific residue thought to be critical for the function under study can then be tested by substitution (2, 3).

A test case using this approach has been the nicotinic acetylcholine receptor (AChR). The *Torpedo californica* AChR is composed of four glycoprotein subunits ( $\alpha, \beta, \gamma, \delta$ )

with stoichiometry  $\alpha_2\beta\gamma\delta$  (4). *In vivo*, the AChR pentamer acts as a ligand-activated cation channel with an effective pore diameter of  $\approx 7$  Å (see ref. 1). A high degree of amino acid sequence homology exists among its four subunits, and each exhibits four presumed transmembrane regions designed as M1, M2, M3, and M4 (5). A synthetic peptide with a sequence that corresponds to M2 $\delta$  forms discrete channels in lipid bilayers. The channel conductance and selectivity sequence are comparable to those characteristic of the authentic AChR channel (2).

This molecular-engineering approach has the great virtue of simplicity. The design, however, dictates that these peptides self-assemble in the membrane to generate discrete conductive oligomers, expressed as channel units. We show here that this lack of control over the final product (oligomeric number) can be circumvented by synthesizing a tethered parallel tetramer with four *Torpedo* AChR M2 $\delta$  peptides attached to a carrier template—a 9-amino acid backbone with four attachment sites (6). When incorporated in lipid bilayers, the complete 101-residue protein forms channels that reproduce several features that are characteristic of authentic AChR channels: single-channel conductance ( $\gamma$ ), cation selectivity, transitions between closed and open states in the millisecond time range, and sensitivity to a local anesthetic channel blocker. Thus, synthetic pore proteins—synporins—provide a strategy to investigate structure-function relationships in channel proteins. A preliminary account of this research was presented elsewhere (7).

### MATERIALS AND METHODS

**Materials.** 1,2-Diphytanoyl-*sn*-glycero-3-phosphocholine (PC), 1-palmitoyl-2-oleyl-*sn*-glycero-3-phosphocholine (POPC), and 1-palmitoyl-2-oleyl-*sn*-glycero-3-phosphoethanolamine (POPE) were obtained from Avanti. All other chemicals were of the highest purity available commercially.

**Synthesis of Proteins.** Synthesis of the four-helix bundles was accomplished by a two-step procedure. A common 9-amino acid template was synthesized using automated solid-phase synthetic techniques starting with 0.5 mmol of *t*-Boc-glycine-PAM resin with a substitution of 0.79 mmol/g (where *t*-Boc is *N*<sup>α</sup>,*N*-*tert*-butyloxycarbonyl; Applied Biosystems). Amino acids (2.0 mmol) were added as the preformed hydroxybenzotriazole (HOBt) esters on an ABI model 431 peptide synthesizer (2, 3). Coupling efficiencies were monitored at all steps by using quantitative ninhydrin assays (8). Coupling steps were repeated as required to generate coupling efficiencies  $\geq 99\%$  per residue. Accordingly, the template NH<sub>2</sub>-K<sup>+</sup>K<sup>+</sup>K<sup>+</sup>PGK<sup>+</sup>E<sup>+</sup>K<sup>+</sup>G-PAM resin was generated, where E<sup>+</sup> is L-glutamic acid,  $\gamma$ -benzyl ester, K<sup>+</sup> is *N*<sup>ε</sup>-2-chlorobenzoyloxycarbonyl-L-lysine, and K<sup>\*</sup> is *N*<sup>ε</sup>-

Abbreviations:  $\gamma$ , single-channel conductance; AChR, acetylcholine receptor; TFE, trifluoroethanol; PC, 1,2-diphytanoyl-*sn*-glycero-3-phosphocholine; POPE, 1-palmitoyl-2-oleyl-*sn*-glycero-3-phosphoethanolamine; POPC, 1-palmitoyl-2-oleyl-*sn*-glycero-3-phosphocholine.

<sup>¶¶</sup>To whom reprint requests should be addressed.

The publication costs of this article were defrayed in part by page charge payment. This article must therefore be hereby marked "advertisement" in accordance with 18 U.S.C. §1734 solely to indicate this fact.

fmoc-L-lysine (fmoc is *N*<sup>ε</sup>-9-fluorenylmethoxycarbonyl). N-terminal lysine was acetylated with 20% (vol/vol) acetic anhydride in dimethylformamide/*N*-methyl pyrrolidone, 70:30 (vol/vol), upon completion of the template synthesis. An aliquot was removed prior to acetylation and the sequence was confirmed by automated Edman chemistry. fmoc groups were then removed using 20% (vol/vol) piperidine in dimethylformamide (20 min). For the second phase, 0.145 mmol of template resin was used to add peptides (Fig. 1A)—AcChoR M2δ, AcChoR [Ala<sup>8</sup>]M2δ (M2δ with Ser-8 → Ala replacement), and AcChoR M1δ. Methods identical to those used for template synthesis were used (2, 3). Multiple couplings (three to five per site) were performed to boost coupling efficiencies to >99% per tetramer unit. Tracer amounts of [<sup>3</sup>H]leucine were added as the *t*-Boc-[<sup>3</sup>H]leucine to leucine-11 of the M2δ peptide to determine concentration in solution. Cleavage and deprotection were carried out in anhydrous HF for 30 min at -10°C and 60 min at 0°C (2, 3).

**Purification of Proteins.** Proteins were subjected to multiple reversed-phase HPLC runs. Proteins were dissolved away from the cleaved resin in CF<sub>3</sub>CH<sub>2</sub>OH (TFE; 99+% pure; Aldrich) and injected onto a Vydac C<sub>4</sub> (semi-prep) 214TP 1010 RP-column equilibrated in 75% buffer A (deionized/distilled water containing 0.1% HPLC-grade trifluoroacetic acid) and 25% buffer B [80% (vol/vol) acetonitrile in water containing 0.1% trifluoroacetic acid]. Proteins were purified through a series of gradient steps followed by 30-min isocratic periods at 55%, 62%, and 75% of solvent B. Samples were reinjected onto a narrow-bore Vydac C<sub>4</sub> RP column 214TP 54 equilibrated as described. Purified channel proteins were eluted by running the column isocratically at 70% of solvent B. Homogeneity was assessed by a third HPLC analysis on the same column and by capillary zone electrophoresis conducted in 20 mM citrate buffer (pH 2.5) at 38°C on an ABI model 270A instrument.

**Amino Acid Analysis and Microsequencing.** Purified peptides (≈1 nmol) were hydrolyzed with 6 M HCl for 1.5 and 3 hr at 165°C *in vacuo*. Samples (in triplicate) were applied to an ABI model 420 amino acid derivatizer and calibrated using

standards provided by the manufacturer. Phenylalanine, lysine, leucine, proline, and valine were used for stoichiometry determination (peptides per template); these residues are stable to the methods employed. All peptides were subjected to sequence analyses multiple times during the purification process using an ABI model 477A automated sequencer with an on-line phenylthiohydantoin amino acid analyzer.

**SDS/PAGE Analysis.** SDS/PAGE analysis was conducted according to Laemmli (9) on 16% tricine gels (Novex, Encinitas, CA). Molecular weight was estimated using CNBr-treated myoglobin molecular weight markers (10). Protein concentration was determined as described (11).

**CD Spectroscopy.** CD spectra were recorded on a JASCO model 600 spectropolarimeter in a 0.1-cm path-length cell. Spectra were recorded in TFE and fitted as described (12).

**Reconstitution in Lipid Bilayers.** Bilayers were formed by apposition of two monolayers at the tip of patch pipettes (13). The lipid [PC or POPE/POPC, 4:1 (wt/wt), in hexane (5 mg/ml)] was spread into monolayers at the air-water interface. The aqueous subphase was composed of 0.5 M NaCl or KCl, 1 mM CaCl<sub>2</sub>, and 10 mM Hepes (pH 7.4). Planar bilayer experiments were performed at 24 ± 1°C. Proteins were incorporated into bilayers by either of two approaches. (i) Protein was extracted from resin (dry weight, 10 mg) in TFE (1 ml). Samples of TFE extract were added to one of the two aqueous compartments separated by a preformed bilayer. Proteins spontaneously inserted into bilayers (final concentration, 300–600 nM) after a time interval of several minutes. (ii) Protein was extracted from resin with a solution of PC (1 mg/ml) in chloroform/methanol, 1:1 (vol/vol), or in hexane. Samples of extract were mixed with membrane-forming solution [either PC or POPE/POPC, 4:1 (wt/wt), at 5 mg/ml in hexane] to achieve final protein/lipid ratios in the range of 1:1000 (wt/wt). The protein/lipid solution in hexane was spread into monolayers at an air-water interface and bilayers were formed (13). Both strategies led to similar channel recordings, thus demonstrating that synporin activity is independent of the pathway used for reconstitution.

#### A TEMPLATE: KR<sup>1</sup>KKR<sup>2</sup>PGKR<sup>3</sup>EKR<sup>4</sup>G

For M2δ, R<sub>i</sub> = EKMSTAI<sup>SVLLAQAVFLLLT</sup>SQR  
 For M2δ S → A, R<sub>i</sub> = EKMSTAI<sup>AVLLAQAVFLLLT</sup>SQR  
 For M1δ R<sub>i</sub> = LFVYIN<sup>FTPCVLISFLASLAF</sup>Y

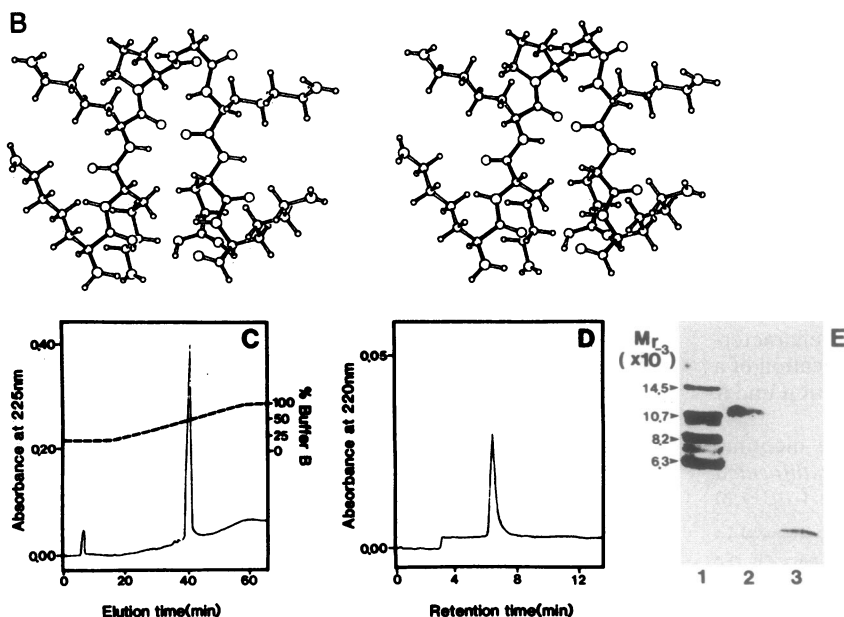


FIG. 1. Chemical characteristics of tetrameric synporins. (A) Amino acid sequence of the multifunctional carrier template (6) and of three 23-mer oligopeptides (2, 7) attached to the template to generate the three synporins studied, M2δ, [Ala<sup>8</sup>]M2δ (M2δ S → A) (with the residues involved in the replacement indicated in bold type), and M1δ. The template shows the four attachment sites; R<sub>i</sub> denotes the oligopeptide anchored to site *i*, where *i* = 1, 2, 3, or 4. Standard one-letter amino acid code is used. (B) Stereoview of a computer-generated molecular model of the template (6). Notice the side chains of the four lysines used as attachment sites and the kink produced by introducing Pro-Gly in the center of the 9-amino acid backbone. Reversed-phase HPLC (C) and capillary zone electrophoresis (D) analysis of tetrameric TM2δ synporin. (E) SDS/PAGE analysis of tetrameric TM2δ synporin. Lanes: 1, molecular weight markers; 2, tetrameric TM2δ; 3, monomeric M2δ. Equivalent results were obtained with tetrameric T[Ala<sup>8</sup>]M2δ and TM1δ.

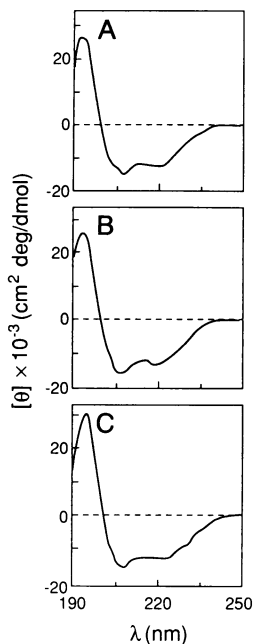


FIG. 2. CD spectra of tetrameric synporins composed of M2 $\delta$  (A), [Ala<sup>8</sup>]M2 $\delta$  (B), and M1 $\delta$  (C) (6.4  $\mu$ M) in TFE (24°C). The parameters of the fitted curves expressed as percentage  $\alpha$ ,  $\beta$ , turn, or random coil are as follows: for TM2 $\delta$ ,  $\alpha$  = 44%,  $\beta$  = 40%, turn = 0, random = 16%; for T[Ala<sup>8</sup>]M2 $\delta$ ,  $\alpha$  = 45%,  $\beta$  = 20%, turn = 0, random = 35%; for TM1 $\delta$ ,  $\alpha$  = 60%,  $\beta$  = 19%, turn = 21%, random = 0.

**Data Acquisition and Analysis.** Electrical recordings and data processing were conducted as described (14, 15). Records were filtered at 2 kHz with an 8-pole Bessel filter (Frequency Devices, Haverhill, MA) and digitized at 100  $\mu$ s per point by using an INDEC-L-11/73-70 microcomputer system (INDEC, Sunnyvale, CA). Analysis was restricted to the most frequent events ( $\geq 80\%$ ) but smaller and larger conductances also occurred at significantly lower frequencies ( $\leq 10\%$ ). Single-channel open and closed conductance levels were discriminated using a pattern-recognition algorithm (15). Conductance values were calculated from the current histogram best fitted by the sum of two Gaussian distributions. Channel lifetimes  $\tau$  were determined by probability density analysis (14, 15); open and closed are denoted by the subscripts O and C, respectively, and subscripts 1 and 2 correspond to the fast and long components of the lifetime distributions, respectively. Data were derived from 58 experiments performed on fresh preparations on different days;  $N$  defines the number of experiments. The total number of events ( $n$ ) analyzed was 28,946; each conductance and life-

time value was determined from analysis of a minimum of 300 events for one point; the maximum  $n$  for one point was 2676;  $\gamma$  and  $\tau$  values are reported as mean  $\pm$  SEM.

## EXPERIMENTAL RESULTS AND DISCUSSION

**Design, Synthesis, and Chemical Characterization of Tetrameric Synporins.** Previous attempts to design transmembrane channels have used bundles of oligo(oxyethylene) chains attached to a polyfunctional macrocyclic polyether (16). The channel activity of these molecules was not evaluated and their biological significance is questionable. Our design follows the principles outlined by Mutter and Villeumier (6): Oligopeptides are tethered to a multifunctional carrier template consisting of a 9-amino acid backbone, K\*KK\*PGK\*EK\*G, with K\* containing *N*<sup>ε</sup>-9-fluorenylmethoxycarbonyl to generate four branch points. Oligopeptides are then attached to the template in a stepwise manner at the 4-base-protected lysine side chains (Fig. 1 A and B). The complete 101-residue proteins are cleaved in HF and purified by reversed-phase HPLC. The amino acid composition, sequence, and purity of the proteins were confirmed by amino acid analysis (hydrolysis with 6 M HCl at 165°C), microsequencing (automated Edman degradation), and analytical HPLC. The proteins were eluted as well-resolved peaks in both HPLC (Fig. 1C) and capillary zone electrophoresis (Fig. 1D). Amino acid analysis further confirmed the predicted stoichiometry of four oligopeptides per template, based on ratios of selected amino acids (e.g., for tetrameric M2 $\delta$ —4 phenylalanines, 9 lysines, 20 leucines, 1 proline, and 8 valines). The three distinct tetrameric proteins migrate in SDS/polyacrylamide gels as single bands with  $M_r \approx 11,000$  (Fig. 1E). This molecular weight is consistent with proteins containing 101 residues. By contrast, the monomer form of M2 $\delta$  migrates with  $M_r \leq 2000$  (Fig. 1E). TM2 $\delta$  is a synporin with four M2 $\delta$  peptides; T[Ala<sup>8</sup>]M2 $\delta$  is an analogue synporin with four [Ala<sup>8</sup>]M2 $\delta$  peptides; TM1 $\delta$  is a protein with four M1 $\delta$  peptides. M1 is a putative transmembrane segment of the AcChoR (5), with amphipathic character, and is postulated to occur at interstices between transmembrane segments and subunits providing extensive hydrophobic contact with the lipid bilayer. However, it is not considered to contribute to the ionic-channel lining and, in fact, M1 $\delta$  peptide mimetics do not form channels in lipid bilayers (2).

**Tetrameric Synporins Are Four-Helix Bundles.** CD spectra show the occurrence of significant  $\alpha$ -helical secondary struc-

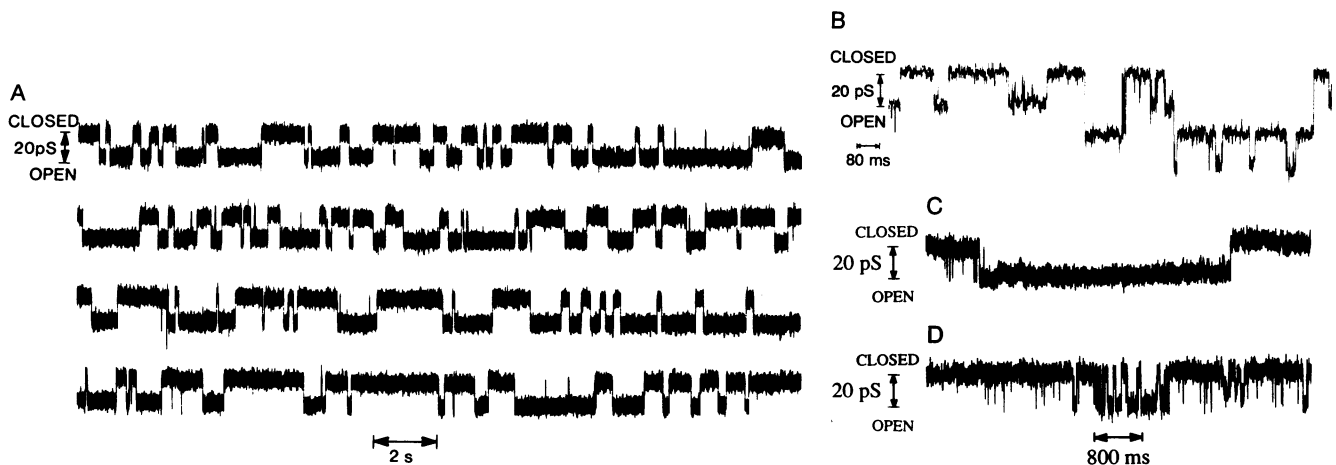


FIG. 3. Single-channel currents from POPE/POPC membranes containing tethered tetrameric M2 $\delta$  synporin in symmetric 0.5 M KCl (pH 7.4) and recorded at 100 mV (A) and 125 mV before (C) and after (D) exposure to 25  $\mu$ M QX-222. Parameters of the fitted probability density functions (14) were  $\tau_{O1}$  = 5 ms,  $\tau_{O2}$  = 581 ms, the ratio of the two amplitudes  $A_1/A_2$  = 0.31 with total number of events analyzed ( $n$ ) = 1530 before exposure to QX-222, and  $\tau_{O1}$  = 4.35 ms,  $\tau_{O2}$  = 50.2 ms,  $A_1/A_2$  = 2.0,  $n$  = 590, after QX-222. (B) Single-channel currents from PC membranes containing monomeric M2 $\delta$ -mimicking peptide in symmetric 0.5 M NaCl (pH 7.2) and recorded at 100 mV. Peptide in TFE was added to the aqueous phase bathing the bilayer at 100 ng/ml.

ture in synporins. Spectra were obtained from solutions of tetrameric synporins in TFE, an organic solvent known to promote helix formation (17). Synporins exhibit the characteristic double minima at  $\approx 222$  nm and  $\approx 208$  nm with a prominent positive peak at  $\approx 195$  nm (Fig. 2). Calculated  $\alpha$ -helical contents for the tetrameric synporins are 44%, 45%, and 60% for M2 $\delta$ , [Ala<sup>8</sup>]M2 $\delta$ , and M1 $\delta$ , respectively.

**Tetrameric M2 $\delta$  Synporins Are Pore Proteins. Ionic conduction.** The tethered tetrameric M2 $\delta$  proteins do indeed form ionic channels in lipid bilayers (Fig. 3A). Currents flowing through single-channel units are clearly resolved as distinct unitary events that fluctuate between open and closed states. Two features are conspicuous in these recordings: the homogeneity of the unitary conductance events and the frequent occurrence of openings lasting several seconds. By contrast, the free M2 $\delta$  23-mer forms channels with heterogeneous conductance amplitudes and open lifetimes (2). This is shown in Fig. 3B where the occurrence of distinct events with  $\gamma = 20$  pS and  $\gamma = 40$  pS is clearly discerned. High-resolution single-channel current recordings from lipid

bilayers containing tetrameric synporins are illustrated in Fig. 4. The single-channel current is calculated from the experimental histograms, which are fitted with the sum of two Gaussian distributions for the closed- and open-channel current levels (14). In PC,  $\gamma$  for the M2 $\delta$  protein in symmetric 0.5 M KCl (Fig. 4A) or 0.5 M NaCl (data not shown) is  $24.3 \pm 1.8$  pS ( $N = 15$ ) and  $18 \pm 1$  pS ( $N = 4$ ), respectively.

**Ionic selectivity.** The channel is cation selective as determined from reversal potential measurements under single salt concentration gradients of KCl or NaCl. Bilayers were formed in the presence of 10-fold salt gradients (0.5 M–0.05 M) and the current–voltage (*I*–*V*) relationships measured between  $-100$  mV and  $100$  mV. The *I*–*V* relations are practically linear. The transference numbers calculated from reversal potential measurements indicate that the pore is cation selective with a  $t^{\text{cation}} \geq 0.96 \pm 0.03$  ( $N = 6$ ). Further, substitution of Cl<sup>-</sup> for aspartate or glutamate does not affect the  $\gamma$  or the reversal potential.

**Channel-gating kinetics.** The M2 $\delta$  synporin forms channels with residence times in the open state that range from the

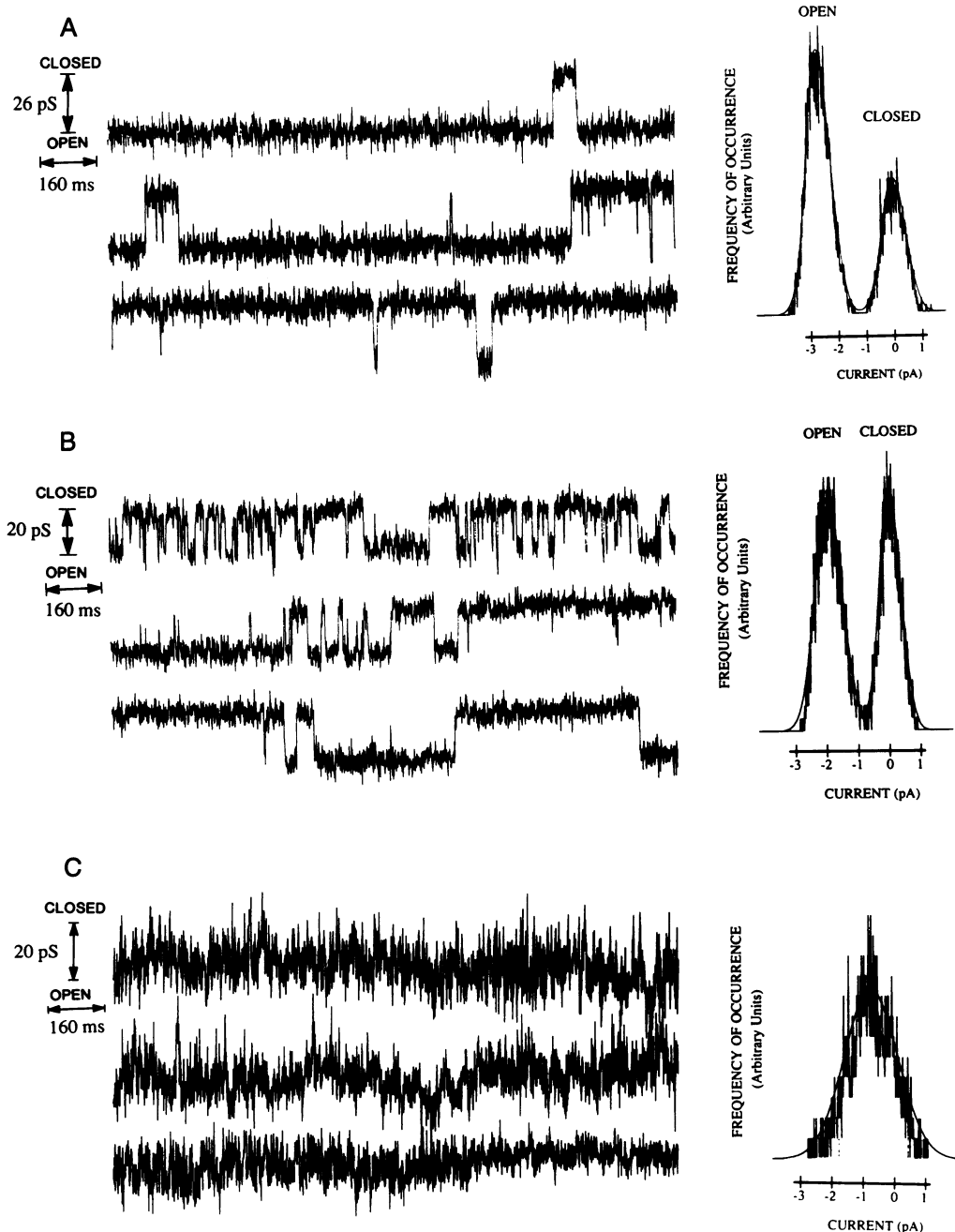


FIG. 4. Single-channel recordings from lipid bilayers containing synthetic channel proteins. Single-channel currents were recorded at 100 mV in symmetric 0.5 M KCl from PC membranes containing tethered tetrameric synporins composed of M2 $\delta$  (A), [Ala<sup>8</sup>]M2 $\delta$  (B), and M1 $\delta$  (C). Single-channel current histograms are shown at the right of the respective records. Fitted Gaussian distributions (smooth curves) correspond to the channel-closed state (peak at zero current) and the open state [peaks at 2.6 pA (A) and 2.0 pA (B)]. Calculated  $\gamma$  values are 26 pS and 20 pS, respectively. No peaks are discernible in C. Other conditions were as for Fig. 3.

millisecond to the second time scale. Single-channel open ( $\tau_O$ ) and closed ( $\tau_C$ ) lifetimes were fitted with the sum of two exponentials (14). The time constants of the fitted curves for symmetric 0.5 M KCl and 0.5 M NaCl solutions are as follows:  $\tau_{O1} = 0.62 \pm 0.31$  ms;  $\tau_{O2} = 67.4 \pm 31$  ms;  $\tau_{C1} = 2.7 \pm 2.1$  ms;  $\tau_{C2} = 294.1 \pm 100$  ms ( $N = 15$ ); and  $\tau_{O1} = 0.9 \pm 0.5$  ms;  $\tau_{O2} = 25.4 \pm 15$  ms;  $\tau_{C1} = 1.2 \pm 0.5$  ms;  $\tau_{C2} = 17 \pm 7$  ms ( $N = 4$ ), respectively.

Thus, the tethered M2 $\delta$  tetramer forms ionic channels in lipid membranes with single-channel properties ( $\gamma$ , cation selectivity, and kinetics of transition between closed and open states) similar to authentic AcChoR channels (1, 13–15).

**Effect of Membrane Lipids.** The  $\gamma$  of tetrameric M2 $\delta$  synporins is affected by the lipid composition of the membrane. Larger  $\gamma$  values in both KCl and NaCl were recorded in bilayers composed exclusively of PC ( $\gamma_{K^+} = 24.3 \pm 1.8$  pS,  $N = 15$ ; and  $\gamma_{Na^+} = 18 \pm 1$  pS,  $N = 4$ ) than in membranes made from POPE/POPC ( $\gamma_{K^+} = 19.9 \pm 0.4$  pS,  $N = 12$ ; and  $\gamma_{Na^+} = 15.0 \pm 0.4$  pS,  $N = 9$ ). However,  $\gamma_{K^+}/\gamma_{Na^+}$  was not altered. This survey, albeit limited, does indicate that the ionic selectivity of the pore structure is primarily determined by its intrinsic characteristics and appears not to be influenced by properties of the host membrane.

**M2 $\delta$  Synporin Analogues Have Different Channel Properties.** A salient advantage offered by designed channel proteins is the opportunity to identify the involvement of specific residues in the processes of ionic conduction through the pore and its selectivity. Accordingly, a tethered M2 $\delta$  tetramer was synthesized in which the Ser-8 was replaced by Ala in each of the four M2 $\delta$  23-mers (Fig. 1). Ser-8 is considered to be exposed to the lumen of the pore and to confer cation selectivity to the authentic AcChoR channel (2, 18–20). This analogue synporin ([Ala<sup>8</sup>]M2 $\delta$ ) does form channels in PC membranes which, however, exhibit a lower  $\gamma$  than M2 $\delta$  synporin:  $20 \pm 1$  pS ( $N = 4$ ) in 0.5 M KCl (Fig. 4B) and  $15.5 \pm 1.3$  pS ( $N = 3$ ) in 0.5 M NaCl (data not shown)—a reduction of 18% in  $\gamma_{K^+}$  and 14% in  $\gamma_{Na^+}$ . The relative  $K^+/Na^+$  selectivity ( $\gamma_{K^+}/\gamma_{Na^+}$ ) of  $\approx 1.4$  of the analogue synporin is practically equivalent to that of M2 $\delta$  synporin ( $\gamma_{K^+}/\gamma_{Na^+} \approx 1.3$ ). A similar reduction of AcChoR  $\gamma$  was recorded in *Xenopus* oocytes injected with mRNA encoding mutant AcChoRs with a Ser  $\rightarrow$  Ala replacement at equivalent positions in the putative M2 segments of the  $\alpha$ ,  $\gamma$ , and  $\delta$  subunits of mouse BC3H-1 AcChoRs (20). The agreement of results obtained by recombinant DNA technology (20, 21) and synthetic protein chemistry (2) validates the proposal that the M2 segments form the AcChoR channel lining and that serines exposed to the pore lumen contribute to the structure of the cationic binding sites (18, 19).

**$\alpha$ -Helical Requirement for Channel Function.** Channel activity of synporins (Figs. 3 and 4) correlates with helix content (Fig. 2). Aging (48–72 hr) or unfolding in 6 M guanidinium chloride reduces both parameters.

**Tetrameric M1 $\delta$  Proteins Do Not Form Channels.** To assess the reliability of the strategy implemented to design channel proteins, a tethered tetramer of M1 $\delta$  23-mers (Fig. 1) was synthesized. M1 $\delta$  tetramers do not produce the unitary conductance steps characteristic of transmembrane channels (Fig. 4C). In contrast, irregular transient fluctuations (spikes) and drifts of membrane conductance along a variable time course without a repeatable characteristic pattern are observed in both 0.5 M KCl ( $N = 7$ ) or 0.5 M NaCl ( $N = 4$ ). Similar activity ( $N = 8$ ) was produced by the 9-amino acid backbone used as template without attached oligopeptides (Fig. 1). Such activity is reminiscent of that generated by hydrophobic and amphiphilic peptides and surfactants that interact with bilayers but do not form well-defined stable transmembrane structures (22). These observations establish a requirement for sequence-specific oligopeptide modules attached to the template for the assembly of ion-conducting pore proteins.

**M2 $\delta$  Synporin Is Blocked by a Local Anesthetic.** To examine the pharmacological specificity of the pore structure generated by the tetrameric M2 $\delta$  synporin, a quaternary derivative (QX-222) of the local anesthetic lidocaine was used. QX-222 is known to transiently block the flow of current through the AcChoR channel, thereby reducing the channel-open lifetime (20, 23). QX-222 also blocks the tetrameric M2 $\delta$  synporin (Fig. 3 C and D). A segment of a record obtained in the absence of QX-222 showing the typical occurrence of brief and long openings is shown in Fig. 3C. After addition of 25  $\mu$ M QX-222, a drastic shortening of channel-open time is evident whereas  $\gamma$  is virtually unaffected (Fig. 3D). Analysis of channel-open lifetimes indicates that the frequency of occurrence of the long openings over the short and their corresponding time constants decreases after exposure to QX-222. The apparent  $K_d$  for blocking is  $\approx 10$   $\mu$ M. Thus, M2 $\delta$  synporin exhibits the sensitivity to local anesthetic channel blockers characteristic of the authentic AcChoR.

We anticipate that the synporin strategy to design pore proteins based on sequence information and oligomeric number will be generally valid and will further our understanding of channel protein function in terms of the underlying structures.

We thank Judy Hempel for kindly providing the molecular model of the template, D. Teplow and J. Racs for the capillary zone electrophoresis studies, John H. Richards for encouragement, and the members of the Montal laboratory for valuable suggestions. This work was supported by grants from Office of Naval Research (N00014-89-J-1469) and U.S. Public Health Service (GM-42340 and MH-44638) and a research scientist award (MH-00778) to M.M., and GM-43617 to J.M.T.

- Hille, B. (1984) *Ionic Channels of Excitable Membranes* (Sinauer, Sunderland, MA), p. 426.
- Oiki, S., Danho, W., Madison, V. & Montal, M. (1988) *Proc. Natl. Acad. Sci. USA* **85**, 8703–8707.
- Oiki, S., Danho, W. & Montal, M. (1988) *Proc. Natl. Acad. Sci. USA* **85**, 2393–2397.
- Reynolds, J. & Karlin, A. (1978) *Biochemistry* **17**, 2035–2038.
- Numa, S. (1989) *Harvey Lect.* **83**, 121–165.
- Mutter, M. & Villeumier, S. (1989) *Angew. Chem. Int. Ed. Engl.* **28**, 535–554.
- Montal, M., Montal, M. S. & Tomich, J. M. (1989) *Soc. Neurosci. Abstr.* **15**, 970.
- Sarin, V. K., Kent, S. B. H., Tam, J. P. & Merrifield, B. (1981) *Anal. Biochem.* **117**, 147–157.
- Laemmli, U. K. (1970) *Nature (London)* **227**, 680–685.
- Kratzin, H. D., Wiltfang, J., Karas, M., Neuhoff, V. & Hilschmann, N. (1989) *Anal. Biochem.* **183**, 1–8.
- Bradford, M. M. (1976) *Anal. Biochem.* **72**, 248–254.
- Henessey, J. P., Jr., & Johnson, W. C. (1981) *Biochemistry* **20**, 1085–1094.
- Suarez-Isla, B. A., Wan, K., Lindstrom, J. & Montal, M. (1983) *Biochemistry* **22**, 2319–2323.
- Labarca, P., Rice, J. A., Fredkin, D. R. & Montal, M. (1985) *Biophys. J.* **47**, 437–441.
- Labarca, P., Lindstrom, J. & Montal, M. (1984) *J. Gen. Physiol.* **83**, 473–496.
- Jullien, L. & Lehn, J.-M. (1988) *Tetrahedron Lett.* **29**, 3803–3806.
- Nelson, J. W. & Kallenbach, N. R. (1986) *Proteins Struct. Funct. Genet.* **1**, 211–217.
- Giraudat, J., Dennis, M., Heidmann, T., Chang, J. Y. & Changeux, J.-P. (1986) *Proc. Natl. Acad. Sci. USA* **83**, 2719–2723.
- Hucho, F., Oberthür, W. & Lottspeich, F. (1986) *FEBS Lett.* **205**, 137–142.
- Leonard, R. J., Labarca, C. G., Charnet, P., Davidson, N. & Lester, H. A. (1988) *Science* **242**, 1578–1581.
- Imoto, K., Busch, C., Sakmann, B., Mishina, M., Konno, T., Nakai, J., Bujo, H., Mori, Y., Fukuda, K. & Numa, S. (1988) *Nature (London)* **335**, 645–648.
- Montal, M. (1976) *Annu. Rev. Biophys. Bioeng.* **5**, 119–175.
- Neher, E. & Steinbach, J. H. (1978) *J. Physiol. (London)* **277**, 153–176.